



## INVESTIGATION OF CATALYTIC BEHAVIOUR OF WO<sub>3</sub> DOPED MAGNETIC DENDRIMERS

Nurdan Kurnaz YETİM<sup>1\*</sup>, Elvan HASANOĞLU ÖZKAN<sup>2</sup>, Mümin Mehmet KOÇ<sup>3,4</sup>

<sup>1</sup>Department of Chemistry, Faculty of Arts and Sciences, Kirkklareli University, Kirkklareli, Türkiye

<sup>2</sup>Department of Chemistry, Faculty of Sciences, Gazi University, Ankara, Türkiye

<sup>3</sup>School of Medical Service, Department of Medical Service and Techniques Kirkklareli University, Kirkklareli, Türkiye

<sup>4</sup>Department of Physics, Faculty of Arts and Sciences, Kirkklareli University, Kirkklareli, Türkiye

### Abstract

In this work, WO<sub>3</sub> nanoparticle decorated magnetic polyamidoamine (PAMAM) dendrimer nanocomposites were fabricated and used as a catalyser for the reduction of 4-nitrophenol (4-NP). Fe<sub>3</sub>O<sub>4</sub> superparamagnetic iron oxide nanoparticles were used as magnetic core. Magnetic iron oxide nanoparticles were produced using co-precipitation method. Magnetic nanoparticle core was covered with PAMAM dendrimers. The dendrimers used in the covering process was 2<sup>nd</sup> generation dendrimers which proposed to protect nanoparticles from losing their magnetic characteristics. PAMAM coated core@shell structure was decorated with WO<sub>3</sub> nanoparticles where Fe<sub>3</sub>O<sub>4</sub>@G2/WO<sub>3</sub> magnetic dendrimer composites were obtained. Structural characterization of magnetic dendrimers was performed using microscopic, spectroscopic and crystallographic methods where SEM, TEM, EDX, XRD methods were used. Vibrating sample magnetometry was used in the assessment of magnetic characteristics. Catalytic performance of the magnetic dendrimers were tracked using UV-vis spectroscopy. Magnetic dendrimers were used for the reduction of 4-NP. Reaction rate coefficient  $k_{app}$  was calculated and found as  $4 \times 10^{-4} \text{ s}^{-1}$ .

**Keywords:** Fe<sub>3</sub>O<sub>4</sub> Nanoparticles; Magnetic Dendrimers; WO<sub>3</sub> Nanoparticles; 4-Nitrophenol

Sorumlu Yazar: Nurdan KURNAZ YETİM, nurdankurnazyetim@klu.edu.tr



## WO<sub>3</sub> KATKILI MANYETİK DENDRIMERLERİN KATALİTİK DAVRANIŞLARININ İNCELENMESİ

### Öz

Bu çalışmada, WO<sub>3</sub> nanoparçacıklar ile dekore edilmiş manyetik poliamidoamin (PAMAM) dendrimerler üretildi ve 4-nitrofenolün indirgenmesi işleminde kullanıldı. Bunun için Fe<sub>3</sub>O<sub>4</sub> süperparamanyetik demir oksit nanoparçacıklar manyetik çekirdek olarak üretildi. Üretimde birlikte çöktürme yöntemi kullanıldı. Manyetik çekirdeğin manyetik özelliğinin kaybolmaması için ikinci jenerasyon PAMAM dendrimerler ile kaplandı. PAMAM kaplı çekirdek@kabuk yapı WO<sub>3</sub> nanoparçacıklar ile dekore edildi ve Fe<sub>3</sub>O<sub>4</sub>@2G/WO<sub>3</sub> manyetik dendrimer nanokompozitler elde edilmiş oldu. Elde edilen yapıların yapısal özellikleri SEM, TEM, EDX, XRD gibi mikroskopik, spektroskopik ve kristalografik metotlar ile incelendi. Manyetik özellikler titreşimli numune magnetometresi ile incelenirken 4-NP UV-vis spektroskopisi ile incelendi. Manyetik dendrimerler 4-NP'nin indirgenmesinde kullanıldı. Tepkime hız sabiti  $k_{app}$  değeri ise  $4 \times 10^{-4} \text{ s}^{-1}$  olarak belirlendi.

**Anahtar Kelimeler:** Fe<sub>3</sub>O<sub>4</sub> Nanoparçacıklar; Manyetik Dendrimerler; WO<sub>3</sub> Nanoparçacıklar; 4-Nitrofenol

### 1. INTRODUCTION

Nanoparticles were used in various medical and engineering applications since they have a unique structure which enables users to tune their characteristics by altering their structure, shape, and size[1]–[3]. Such alteration often leads to a drastic change in optic, electronic, catalytic, and magnetic properties [1]–[5]. Up to now, various types of nanoparticles were reported. Among those, metallic nanoparticles were found to be quite interesting since they can provide paramount characteristics which make them suitable candidates for catalytic, electronic and optoelectronic applications[5], [6]. Metallic nanoparticles have high electron density with low electron affinity. Some metal nanoparticles illustrate ferromagnetic or superparamagnetic characteristics which made them a suitable candidate for magnetic applications[4], [7]. Different forms of nanoparticles such as nanocomposites, nanoalloys, nanofilms, nanocubes, *etc.* were reported in the literature [5]. Nanocomposites are smart nanotools which can exhibit multifunctional characteristics. For example, nanocomposites can illustrate good magnetic and catalytic properties with high stability. To be able to do this, magnetic nanoparticle core such as Fe<sub>3</sub>O<sub>4</sub>, Co<sub>3</sub>O<sub>4</sub>, NiO, *etc.* were often



preferred [8]–[10]. In this regard,  $\text{Fe}_3\text{O}_4$  nanoparticles are a good candidate as core material illustrates outstanding magnetic saturation with low coercivity [11]. Covering such a magnetic core with protective organic shell layer often provides stability in magnetic characteristics, since the a protective layer limits interaction with the surrounding environment [6], [12]. Different organic molecules or dendrimers were used as shell layers in core@shell structures. The shell layer can also be doped with different molecules and/or nanoparticles which enables inorganic-organic core@shell structure to be functionalized [6], [12]. Where multifunctional properties could be obtained. Decorating magnetic core@shell structure with material with high catalytic properties can enable us to obtain functionalized magnetic nanocomposites.

In this regard, magnetic nanocomposites have the potential to be used in catalytic applications. Catalytic materials are needed for different applications and can be applied in different fields, antimicrobial applications, environmental applications, medical applications, *etc.* Organic and inorganic pollutants are often released to nature and degradation and/or reduction of such compounds were needed for a better, cleaner, and healthier environment. Nitrophenol-based compounds were found in industrial and agricultural waste waters and were known as common organic pollutants [13], [14]. Degradation and/or removal of nitrophenol-based products from waters were found to be expensive and compelling [13], [14]. Nitrophenol derivatives are also toxic to the marine life, ecosystem and living organisms [15], [16]. Nitro derivatives should be degraded or reduced to amine-based derivatives since such derivatives could naturally be decomposed or biologically degraded [15], [17]. 4-nitrophenol (4-NP) is vastly used in different industrial products and is often produced as an intermediate product. To reduce the toxic and deleterious effects of 4-NP, it should be reduced to 4-aminophenol (4-AP). Such a reduction process may be difficult and/or costly. Catalytic materials could help users to speed up the reduction process with minimum cost. In this regard, metal based nanoparticles provide promising, fast, reliable results with minimum production and operation costs [18]–[22].

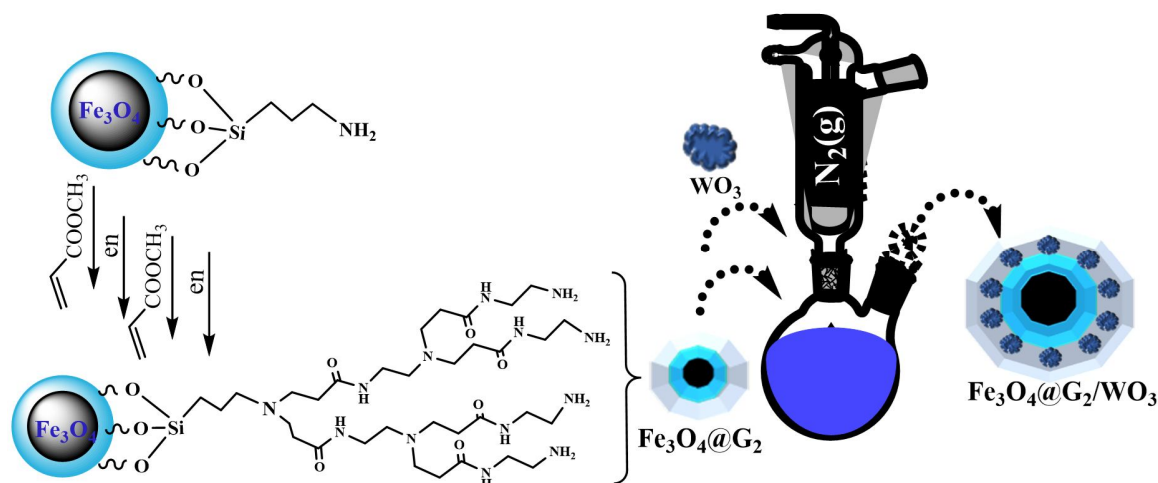


**Figure 1.** Fabrication of  $\text{Fe}_3\text{O}_4@\text{G}_2/\text{WO}_3$  magnetic nanocomposites.

In our work, we produced functional  $\text{Fe}_3\text{O}_4@\text{G}_2/\text{WO}_3$  magnetic nanocomposites and used them as a potential catalyser for the reduction of 4-NP to 4-AP. In our previous studies, we managed to produce  $\text{Fe}_3\text{O}_4$  magnetic nanoparticles with a high saturation rate [17], [23]. We used such magnetic nanoparticles as magnetic core and covered them with 2<sup>nd</sup> generation PAMAM dendrimers [23], [24]. Core@shell structure was decorated with  $\text{WO}_3$  nanoparticles where novel  $\text{Fe}_3\text{O}_4@2\text{G}/\text{WO}_3$  magnetic nanocomposites were obtained with good catalytic properties. Structural characterization of the nanoparticles was performed with the scanning electron microscope (SEM) equipped with energy dispersive X-ray spectra (EDX) apparatus. X-ray diffractometry was also used for crystallographic characterization. The catalytic activities were investigated using UV-vis spectroscopy. The catalytic performance of novel multifunctional nanocomposite was assessed, and the results were compared with the results previously reported in the literature.

## 2. MATERIALS AND METHOD

### 2.1. Materials and Reagents

Tungsten (VI) oxide nanopowders (with nanoparticle size < 100 nm) was obtained from Sigma-Aldrich. Chemical reagents such as 3-Aminopropyl triethoxysilane (APTES), iron salts ( $\text{FeCl}_3 \cdot 6\text{H}_2\text{O}$  and  $\text{FeCl}_2 \cdot 4\text{H}_2\text{O}$ ), methylacrylate, tetraethylortasilicate (TEOS), 28% ammonia



(NH<sub>3</sub>), ethylenediamine, methanol, ethanol, were purchased from Sigma-Aldrich.

## 2.2. Synthesis of Fe<sub>3</sub>O<sub>4</sub>@G2/WO<sub>3</sub> Magnetic Dendrimer

Fe<sub>3</sub>O<sub>4</sub> magnetic nanoparticles used as a core was produced according to the method we previously describe in our previous reports [23], [24]. Fe<sub>3</sub>O<sub>4</sub> magnetic core was covered with 2<sup>nd</sup> generation PAMAM dendrimers and Fe<sub>3</sub>O<sub>4</sub>@G2 PAMAM structures were obtained. To decorate the core@shell structure 0.2 g Fe<sub>3</sub>O<sub>4</sub>@G2 PAMAM was dissolved in 20 mL methanol and sonicated for 20 min. 20 mg of WO<sub>3</sub> nanopowder was added to the suspension and the suspension was stirred for 24 h under nitrogen flow. As a result, novel Fe<sub>3</sub>O<sub>4</sub>@G2/WO<sub>3</sub> multi-functional nanocomposites were obtained. Nanocomposites were collected using a magnet. Nanocomposite powder was washed with ethanol and pure water and kept in over for 12 h at 40°C. Please see the Figure 1 for the detailed schematics of the production.

## 3. RESULT AND DISCUSSION

### 3.1. Characterization of Fe<sub>3</sub>O<sub>4</sub>@G2/WO<sub>3</sub> Nanocomposites

Results about Fe<sub>3</sub>O<sub>4</sub> magnetic core and Fe<sub>3</sub>O<sub>4</sub>@2G structures were discussed in our previous reports where results pertaining to FTIR, XRD, TGA, VSM, and different elemental analysis methods were provided [11], [23], [24]. In this section, the characterization of Fe<sub>3</sub>O<sub>4</sub>@G2/WO<sub>3</sub> nanoparticle composites will be discussed. Figure 2 illustrates EDX spectrum and SEM image of Fe<sub>3</sub>O<sub>4</sub>@G2/WO<sub>3</sub> nanocomposites. EDX spectrum illustrates apparent Fe, O, W, and C peaks. Si and N peaks that appeared in the spectrum are related to TEOS and APTES support. SEM image shows Fe<sub>3</sub>O<sub>4</sub>@G2/WO<sub>3</sub> nanocomposites. As can be seen from the image, nanocomposites were in granulated form. The particle size was found to be around 100 nm. To confirm the nanostructure in detail, TEM images of the nanocomposites were also obtained.

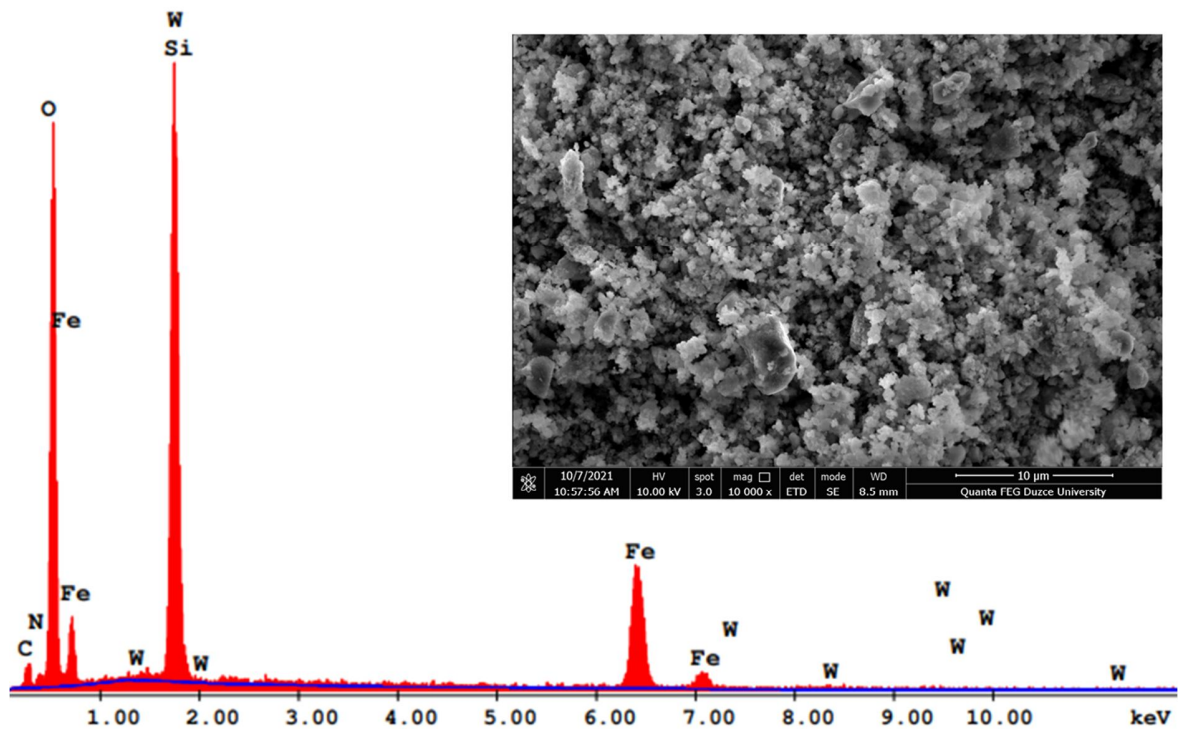


**Figure 2.** SEM image and EDX spectrum and SEM image of Fe<sub>3</sub>O<sub>4</sub>@G2/WO<sub>3</sub> nanocomposites

TEM image of the Fe<sub>3</sub>O<sub>4</sub>@G2/WO<sub>3</sub> nanocomposites were illustrated in Figure 3. The figure also confirms the granulated form of the nanocomposites. Granulated parts seemed to be clustered where agglomerated clusters could be seen. Also, very dark, dark, and light sections could be seen in the figure. In the branched clusters, dark sections could be seen inside where lighter clusters covers them. Darker sections were thought to be Fe<sub>3</sub>O<sub>4</sub> magnetic cores. The very dark sections placed outside of the branched clusters were thought to be WO<sub>3</sub> nanoparticles. Lighter parts around darker spheres are organic shells consisting of PAMAM, APTES and TEOS. The size of the nanoparticles in the dendritic structure alters where the Fe<sub>3</sub>O<sub>4</sub> nanoparticles were found to be around 10-20 nm. The WO<sub>3</sub> nanoparticles were found to be around 20 nm. Nanocomposites consisting of agglomerated nanoparticles and organic dendrimers were measured around 100 nm. Nanocomposites were found to be agglomerated form. Since PAMAM dendrimers are in branchy structure, nanoparticles are stuck between organic branches and tend to agglomerate. The branches also tend to stick to each other where slightly bigger chain like cluster groups were formed.

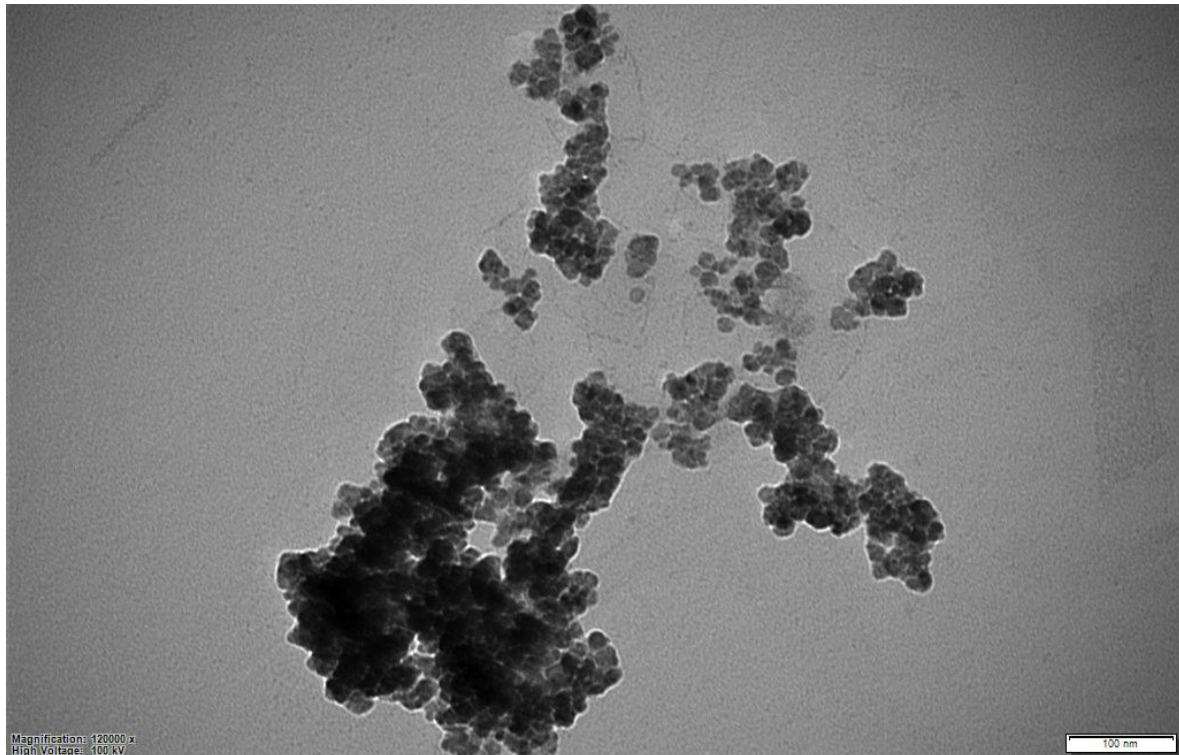


**Figure 3.** TEM images of  $\text{Fe}_3\text{O}_4@\text{G2}/\text{WO}_3$

Magnetic characteristics of the iron (II/III) oxide core and  $\text{Fe}_3\text{O}_4@\text{G2}/\text{WO}_3$  nanocomposites were investigated using vibrating sample magnetometry (VSM). Figure 4 illustrates VSM results of  $\text{Fe}_3\text{O}_4$  and  $\text{Fe}_3\text{O}_4@\text{G2}/\text{WO}_3$  nanocomposites. VSM plots of the iron oxide core and magnetic nanocomposites exhibit superparamagnetic characteristics where almost no coercivity was observed for each sample. The magnetic saturation value of the magnetic iron (II/III) oxide core was found as 63.7 emu/g while the magnetic saturation value of the magnetic nanocomposites was found as 22.9 emu/g. A dramatic decrease in magnetic saturation value was obtained after covering magnetic nanoparticles with PAMAM dendrimers and decorating them with  $\text{WO}_3$  nanoparticles. It is highly possible that covering iron oxide nanoparticles with the outer shell and decorating them with  $\text{WO}_3$  change their electronic structure which causes a rapid decrease in magnetic saturation values. It was seen that our magnetic nanoparticles exhibit outstanding magnetic characteristics where the saturation value of the nanoparticles was found to be quite high compared to the different organic-inorganic core@multi-shell nanocomposites.

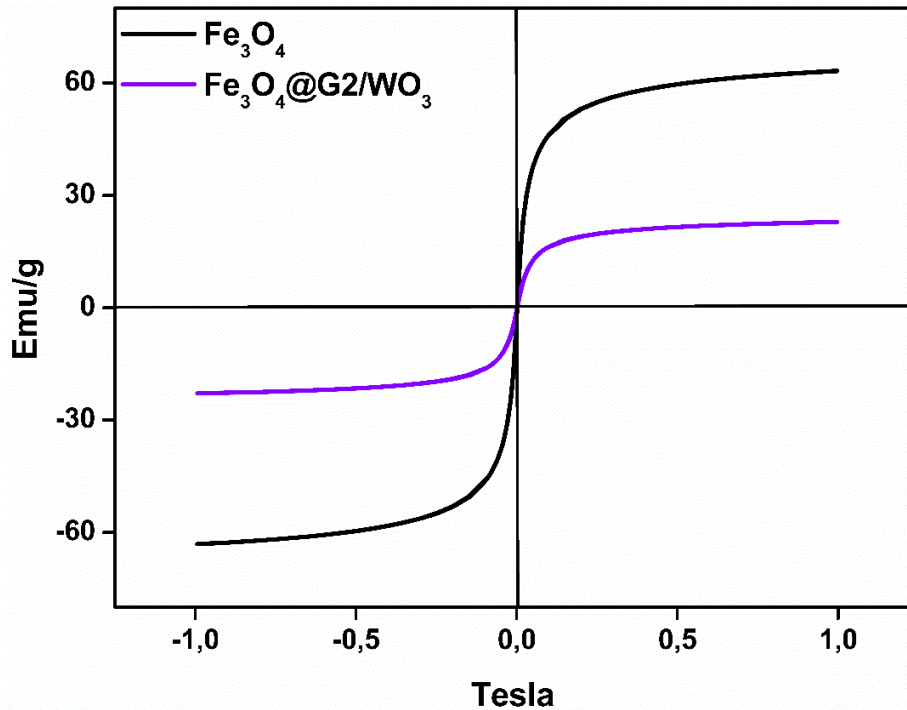


**Figure 4.** Magnetic hysteresis of  $\text{Fe}_3\text{O}_4$  and  $\text{Fe}_3\text{O}_4@\text{G2}/\text{WO}_3$  magnetic nanocomposite

**Table 1:** Comparison of magnetic saturation values

Sample	Magnetic Saturation Values (emu/g)	Reference
$\text{Fe}_3\text{O}_4$	63.7	[23]
$\text{Fe}_3\text{O}_4@\text{SiO}_2$	48.7	[23]
$\text{Fe}_3\text{O}_4@\text{G2}$	34.7	[23]
$\text{Fe}_3\text{O}_4@\text{G2}/\text{WO}_3$	22.90	TW

*TW: This work*

### 3.2. Catalytic Activity

The catalytic performance of the  $\text{Fe}_3\text{O}_4$  nanoparticle core for the degradation of 4-NP to 4-AP was assessed in our previous studies [23]. In this work, the catalytic performance of  $\text{Fe}_3\text{O}_4@\text{G2}/\text{WO}_3$



magnetic nanocomposites was assessed for the reduction of 4-NP to 4-AP in the presence of  $\text{NaBH}_4$ . In the catalytic reaction, 10 mg of  $\text{Fe}_3\text{O}_4@\text{G2}/\text{WO}_3$  magnetic nanocomposites were used as a catalyser for the reduction of 0.1 mM 4-NP where 0.2 mM  $\text{NaBH}_4$  was used as support material. The catalytic reaction was tracked using UV-vis spectrometry. UV-vis spectroscopy consecutively scans the solution. The schematic illustrating the experimental procedure was presented in Figure 5. For the initial scan. A peak related to the 4-NP was seen in the absorbance spectra at around 400 nm. The peak is a 4-NP related peak, and the peak strength is related to the concentration of 4-NP. After the presence of  $\text{NaBH}_4$ , a sudden peak appears around 310 nm. The peak at 310 nm is a 4-AP related peak indicating the existence of 4-AP. However, in the measurement where no catalyser was added to the solution the intensity of the peak at 400 nm did not change. The case indicates that the peak at 400 nm is definitely related to the 4-NP. In addition, the strong peak at 325 nm illustrates that 4-NP is directly reduced to 4-AP without any side reaction. Figure 5 illustrates the reaction mechanism and the measurement process.

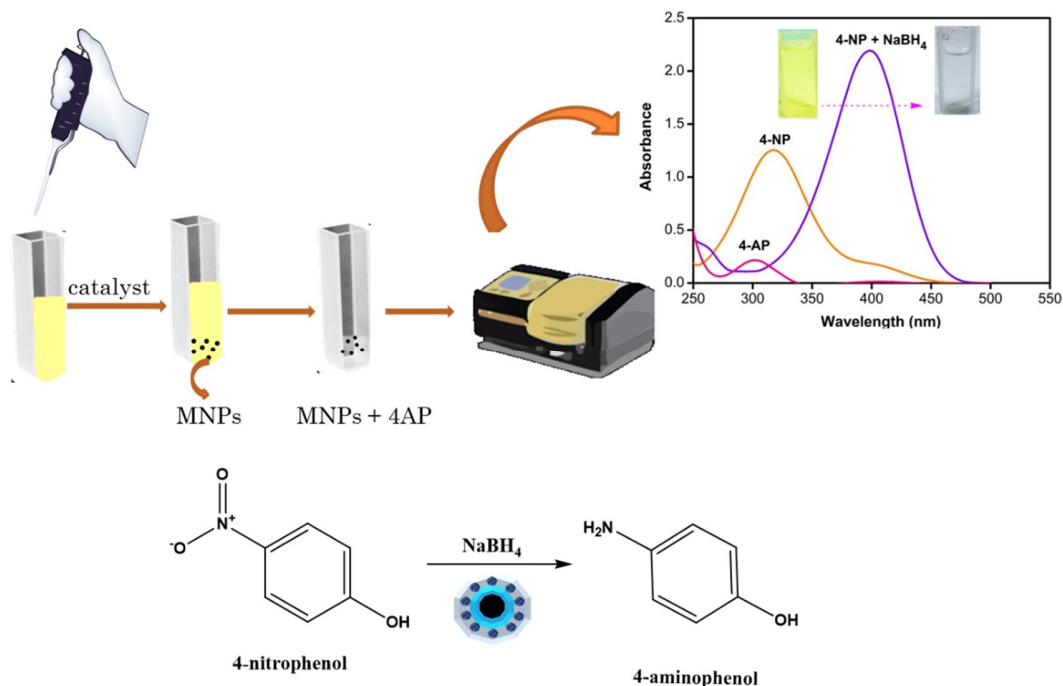


**Figure 5.** Experimental process and reduction of 4-NP to 4-AP was illustrated in the figure.

UV-vis spectrum related to the reduction process for  $\text{Fe}_3\text{O}_4@\text{G2}/\text{WO}_3$  magnetic nanocomposites were illustrated in Figure 6. 1h later of addition of  $\text{Fe}_3\text{O}_4@\text{G2}/\text{WO}_3$  nanocomposites 89% of the

reduction process was completed. In the catalysis reaction, NaBH<sub>4</sub> concentration was found to be much higher than 4-NP; therefore, NaBH<sub>4</sub> concentration was assumed to be stable during the reaction. Hence, the catalysis reaction should be accepted as a first order pseudo reaction which depends on the concentration of 4-NP. Catalysis reaction was accepted as a first order reaction since ln (A<sub>t</sub>/A<sub>0</sub>) is a time dependent reaction. Thus, Eq.1, Eq.2 and Eq.3 were used to assess the reaction rate coefficient “k”.

$$\vartheta = dC/dt = -k * C^n \tag{Eq.1}$$

n = 1 assuming;

$$\int_{C_0}^{C_t} dC/C = -k \int_0^t dt \tag{Eq.2}$$

$$\ln\left(\frac{C_t}{C_0}\right) = \ln\left(\frac{A_t}{A_0}\right) = -k * t \tag{Eq.3}$$

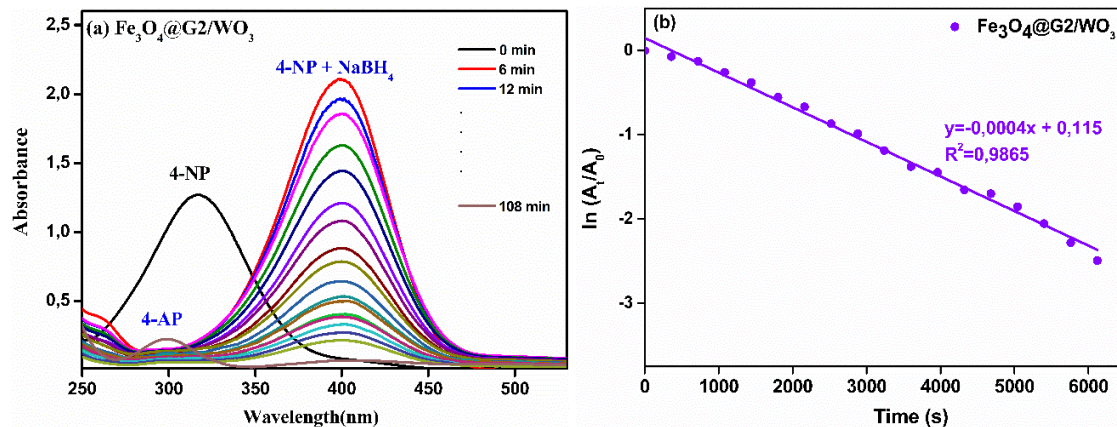
where  $\vartheta$  reaction speed, n reaction order, C<sub>t</sub> time dependent concentration, C<sub>0</sub> initial reaction, k reaction rate coefficient, t time, A<sub>t</sub> time related absorbance value, A<sub>0</sub> is the absorbance value when t= 0.

Figure 6b illustrates a time related ln(A<sub>t</sub>/A<sub>0</sub>) plot where the reaction rate coefficient was able to be calculated. The reaction rate of our nanoparticles and similar results in the literature was presented in Table 1. For Fe<sub>3</sub>O<sub>4</sub>@G2/WO<sub>3</sub> nanoparticles, the reaction rate  $k_{app}$  was defined as 4x10<sup>-4</sup> s<sup>-1</sup>. It was seen that the reaction rate obtained by the Fe<sub>3</sub>O<sub>4</sub>@G2/WO<sub>3</sub> nanoparticles for the reduction of 4-NP to 4-AP is much better than the results previously reported in the literature. It was found that our nanoparticles exhibit outstanding catalytic performance with magnetic properties that magnetic nanoparticles could easily be collected from the solution via magnets.

**Table 2.** Comparison of the results of this work with other reported methods in the reduction of 4-NP to 4-AP.

Catalyst	The amount of catalyst	4-NP	NaBH <sub>4</sub>	$k_{app}$	Ref.
Fe <sub>3</sub> O <sub>4</sub> @PS@PAMAM-Ag	10 mg	0.015 g/L	4 g/L	0.131 min <sup>-1</sup>	[25]
Ag-DENs	5 μM	600 μM	0.1 M	2.51x10 <sup>-2</sup> s <sup>-1</sup>	[26]
Fe <sub>3</sub> O <sub>4</sub> @CS-Starch/Pd	0.01 mol%	2.5 mM	0.25 mM	0.58 min <sup>-1</sup>	[27]
Fe <sub>3</sub> O <sub>4</sub> @G2/WO <sub>3</sub>	10 mg	0.1 mM	0.2 M	4x10 <sup>-4</sup> s <sup>-1</sup>	TW

TW: This work



**Figure 6.** UV–vis spectra obtained in the 4-NP reduction in the presence of Fe<sub>3</sub>O<sub>4</sub>@G2/WO<sub>3</sub> (a) nanostructures and plot of the  $\ln(A_t/A_0)$  against the reaction time (b)

#### 4. CONCLUSION

In this work, we managed to produce Fe<sub>3</sub>O<sub>4</sub>@G2/WO<sub>3</sub> nanocomposites. Nanocomposites consisting of iron oxide magnetic superparamagnetic core which was covered with organic PAMAM shell and decorated with WO<sub>3</sub> nanoparticles. Structural characteristics of the nanocomposites were confirmed where the dendritic structure was achieved with magnetic characteristics. VSM results illustrate that the magnetic core has 63.7 emu/gr magnetic saturation rate whereas Fe<sub>3</sub>O<sub>4</sub>@G2/WO<sub>3</sub> has 22.9 emu/gr magnetic saturation rate. It was seen that covering the magnetic core with organic molecules and decorating it with WO<sub>3</sub> decreased the overall saturation rate. We compared our results with the results reported in the literature. Our results show that our nanocomposites have still relatively high magnetic saturation rates. Magnetic saturation rates of our nanoparticles were found to be higher than similar magnetic nanoparticles previously reported in the literature. The catalytic performance of the nanoparticles was assessed for the reduction of 4-NP to 4-AP. It was concluded that nanocomposites exhibit good catalytic performance. In our work, we compared the reaction rate coefficient of the nanocomposites with the reported works. We found our nanoparticles exhibit better performance than similar nanoparticles and nanocomposites which were reported in the literature. It was concluded that our nanocomposites are multifunctional materials, and they illustrated astonishing catalytic performance with outstanding magnetic characteristics.



## 5. ACKNOWLEDGEMENT

This study was supported by Kirkklareli University Scientific Research Projects Coordination Unit. Project number: KLÜBAP 236 and KLÜBAP 229.

## REFERENCES

- [1] M. M. Koç and G. E. Ragkousis, AFM induced diffusion of large scale mobile HOPG defects, *Appl. Nanosci.*, vol. 9, no. 7, 2019.
- [2] D. Vikraman and H. J. Park, Shape-selective synthesis of NiO nanostructures for hydrazine oxidation as a nonenzymatic amperometric sensor, *RSC Adv.*, vol. 6, no. 89, pp. 86101–86107, Sep. 2016.
- [3] S. A. Kulkarni, P. S. Sawadh, P. K. Palei, and K. K. Kokate, Effect of synthesis route on the structural, optical and magnetic properties of Fe<sub>3</sub>O<sub>4</sub> nanoparticles, *Ceram. Int.*, vol. 40, no. 1 PART B, pp. 1945–1949, Jan. 2014.
- [4] C. Binns et al., Preparation of hydrosol suspensions of elemental and core-shell nanoparticles by co-deposition with water vapour from the gas-phase in ultra-high vacuum conditions, *J. Nanoparticle Res.*, vol. 14, no. 9, p. 1136, Aug. 2012.
- [5] E. Roduner, Size matters: Why nanomaterials are different, *Chem. Soc. Rev.*, vol. 35, no. 7, pp. 583–592, Jun. 2006.
- [6] N. Aslan, B. Ceylan, M. M. Koç, and F. Findik, Metallic nanoparticles as X-Ray computed tomography (CT) contrast agents: A review, *J. Mol. Struct.*, vol. 1219, p. 128599, Nov. 2020.
- [7] S. Aktas, S. C. Thornton, C. Binns, and P. Denby, Gas phase synthesis of core-shell Fe@FeO x magnetic nanoparticles into fluids, *J. Nanoparticle Res.*, vol. 118, p. 365, 2016.
- [8] J. Safaei-Ghomi and F. Eshteghal, Nano-Fe<sub>3</sub>O<sub>4</sub>/PEG/succinic anhydride: A novel and efficient catalyst for the synthesis of benzoxanthenes under ultrasonic irradiation, *Ultrason. Sonochem.*, vol. 38, pp. 488–495, Sep. 2017.
- [9] S. R. Krishnakumar et al., Magnetic linear dichroism studies of in situ grown NiO thin films, *J. Magn. Magn. Mater.*, vol. 310, no. 1, pp. 8–12, Mar. 2007.
- [10] Y. Zhang, Y. Chen, T. Wang, J. Zhou, and Y. Zhao, Synthesis and magnetic properties of nanoporous Co<sub>3</sub>O<sub>4</sub> nanoflowers, *Microporous Mesoporous Mater.*, vol. 114, no. 1–3, pp. 257–261, Sep. 2008.
- [11] N. Kurnaz Yetim, F. Kurşun Baysak, M. M. Koç, and D. Nartop, Characterization of magnetic Fe<sub>3</sub>O<sub>4</sub>@SiO<sub>2</sub> nanoparticles with fluorescent properties for potential multipurpose imaging and theranostic applications, *J. Mater. Sci. Mater. Electron.*, vol. 31, no. 20, pp. 18278–18288, 2020.



- [12] M. M. Koç, N. Aslan, A. P. Kao, and A. H. Barber, Evaluation of X-ray tomography contrast agents: A review of production, protocols, and biological applications, *Microsc. Res. Tech.*, vol. 82, no. 6, 2019.
- [13] J. Luan and A. Plaisier, Study on treatment of wastewater containing nitrophenol compounds by liquid membrane process, *J. Memb. Sci.*, vol. 229, no. 1–2, pp. 235–239, Feb. 2004.
- [14] Z. D. Pozun et al., A systematic investigation of p -nitrophenol reduction by bimetallic dendrimer encapsulated nanoparticles, *J. Phys. Chem. C*, vol. 117, no. 15, pp. 7598–7604, Apr. 2013.
- [15] N. Kurnaz Yetim, N. Aslan, and M. M. Koç, Structural and catalytic properties of Fe<sub>3</sub>O<sub>4</sub> doped Bi<sub>2</sub>S<sub>3</sub> novel magnetic nanocomposites: P-Nitrophenol case, *J. Environ. Chem. Eng.*, vol. 8, no. 5, p. 104258, 2020.
- [16] A. Serrà, R. Artal, M. Pozo, J. Garcia-Amorós, and E. Gómez, Simple Environmentally-Friendly Reduction of 4-Nitrophenol, *Catal. 2020*, Vol. 10, Page 458, vol. 10, no. 4, p. 458, Apr. 2020.
- [17] N. Kurnaz Yetim and E. Hasanoğlu Özkan, Synthesis of Au-doped magnetic nanocomposites: structural, magnetic, and catalytic properties, *J. Mater. Sci. Mater. Electron.*, vol. 32, no. 20, pp. 24766–24774, Oct. 2021.
- [18] C. Pan et al., “Facile fabrication of steam-exploded poplar loaded with non-metal-doped Ni-Fe nanoparticles: Catalytic activities in 4-nitrophenol reduction and electrocatalytic reaction,” *Arab. J. Chem.*, vol. 15, no. 7, p. 103944, Jul. 2022.
- [19] K. Saravanakumar, V. S. Priya, V. Balakumar, S. L. Prabavathi, and V. Muthuraj, Noble metal nanoparticles (Mx = Ag, Au, Pd) decorated graphitic carbon nitride nanosheets for ultrafast catalytic reduction of anthropogenic pollutant, 4-nitrophenol, *Environ. Res.*, vol. 212, p. 113185, Sep. 2022.
- [20] X. Liu et al., Microwave-assisted synthesis of 2D Zr-MOF nanosheets supported gold nanocomposites as efficient catalysts for the reduction of 4-nitrophenol, *J. Alloys Compd.*, vol. 922, p. 165939, Nov. 2022.
- [21] N. Sahiner, A. Kaynak, and S. Butun, Soft hydrogels for dual use: Template for metal nanoparticle synthesis and a reactor in the reduction of nitrophenols, *J. Non. Cryst. Solids*, vol. 358, no. 4, pp. 758–764, Feb. 2012.
- [22] G. Kibar and D. Ş. Ö. Dinç, In-situ growth of Ag on mussel-inspired polydopamine@poly(M-POSS) hybrid nanoparticles and their catalytic activity, *J. Environ. Chem. Eng.*, vol. 7, no. 5, p. 103435, Oct. 2019.
- [23] N. Kurnaz Yetim, M. M. Koç, and D. Nartop, Magnetic dendrimer-encapsulated metal nanoparticles (Au, Ag): effect of dendrimerization on catalytic reduction of 4-nitrophenol, *J. Iran. Chem. Soc.*, vol. 19, no. 6, pp. 2569–2580, Jun. 2022.



- [24] N. Kurnaz Yetim, F. Kurşun Baysak, M. M. Koç, and D. Nartop, Synthesis and characterization of Au and Bi<sub>2</sub>O<sub>3</sub> decorated Fe<sub>3</sub>O<sub>4</sub>@PAMAM dendrimer nanocomposites for medical applications, *J. Nanostructure Chem.*, vol. 11, pp. 589–599, Feb. 2021.
- [25] G. Dang, Y. Shi, Z. Fu, W. Yang, Fe<sub>3</sub>O<sub>4</sub>@PS@PAMAM-Ag Magnetic Nanocatalysts and Their Recoverable Catalytic Ability, *Chin. J. Catal.*, vol. 33, pp. 651–658, April. 2012.
- [26] M. Nemanashi, R. Meijboom, Synthesis and characterization of Cu, Ag and Au dendrimer-encapsulated nanoparticles and their application in the reduction of 4-nitrophenol to 4-aminophenol, *J. Colloid Interface Sci.*, vol. 389, pp. 260–267, Jan. 2013.
- [27] H. Veisi, Z. Joshani, B. Karmakar, T. Tamoradi, M. M. Heravi, and J. Gholami, Ultrasound assisted synthesis of Pd NPs decorated chitosan-starch functionalized Fe<sub>3</sub>O<sub>4</sub> nanocomposite catalyst towards Suzuki-Miyaura coupling and reduction of 4-nitrophenol, *Int. J. Biol. Macromol.*, vol. 172, pp. 104–113, Mar. 2021.